PERGAMON

International Journal of Heat and Mass Transfer 45 (2002) 765–773

International Journal of HEAT and MASS TRANSFER

www.elsevier.com/locate/ijhmt

Heat transfer in rectangular microchannels

Gokturk Tunc, Yildiz Bayazitoglu *

Mechanical Engineering and Materials Science Department, Rice University, 6100 Main Street, MS 321, Houston, TX 77005-1892, USA

Received 27 December 2000; received in revised form 4 June 2001

Abstract

Convection heat transfer in a rectangular microchannel is investigated. The flow is assumed to be fully developed both thermally and hydrodynamically. The H2-type boundary condition, constant axial and peripheral heat flux, is applied at the walls of the channel. Since the velocity profile for a rectangular channel is not known under the slip flow conditions, the momentum equation is first solved for velocity. The resulting velocity profile is then substituted into the energy equation. The integral transform technique is applied twice, once for velocity and once for temperature. The results show a similar behavior to previous studies on circular microtubes. The values of the Nusselt number are given for varying aspect ratios. © 2001 Published by Elsevier Science Ltd.

1. Introduction

Microscale heat transfer has been gaining more interest as the size of the devices decreases, as in electronic devices, since the amount of heat that needs to be dissipated per unit area increases. The performance of these devices is directly related to the temperature, therefore it is a critical issue to keep the temperature within certain limits.

As the size of a channel is reduced, the continuum flow assumption is no longer valid, however there is a certain value for the size that one can still apply Navier–Stokes equations with some modifications on the boundary conditions [1,2]. The flow in these conditions is called slip flow. Knudsen number is defined to represent the rarefaction effects. It is the ratio of the mean free path to the characteristic length of the channel. Beskok et al. [3] give the range for the Knudsen number in slip-flow regime as $0.001 < Kn < 0.1$.

Velocity slip and temperature jump are the two major effects of rarefaction. These are quantified by using the Knudsen number. In this study, to represent the velocity slip, a parameter called "slip coefficient" was defined as the ratio of the velocity of the fluid at the wall to the mean velocity. The variation of this parameter with the Knudsen number will be shown for different aspect ratios.

Convection heat transfer in rectangular macrochannels has been solved by numerical and analytical means over the years [4–6]. No attempt has been made, however for solving the same problem in microchannels, although the solution for microtubes is available in the literature. Flow in a microtube was investigated by several researchers [7–10]. In these studies, the effects of velocity slip and temperature jump at the wall and viscous heating in the medium were considered. The main finding was that velocity slip and temperature jump have opposite effects on heat transfer. While the velocity slip tends to increase the Nusselt number, the temperature jump tends to decrease it. The inclusion the viscous heating increases the Nusselt number for the fluid being cooled and decreases it for the fluid being heated. In these analyses both uniform temperature and uniform heat flux boundary conditions were considered. The results were published for the thermal entrance region as well as for fully developed flow.

The aim of this analysis is to obtain the temperature profile and thus the Nusselt number for varying values of the aspect ratio in a microchannel. To obtain the temperature distribution, one needs to solve for velocity first. Since there is no such literature available for fully developed velocity profile, including the velocity slip at the wall, the integral transform technique was first

* Corresponding author. Tel.: +1-713-348-6291; fax: +1-713-348-5423.

E-mail address: bayaz@rice.edu (Y. Bayazitoglu).

0017-9310/02/$ - see front matter © 2001 Published by Elsevier Science Ltd.
PII: S0017-9310(01)00201-0

Nomenclature

a	long side of the channel
$A_n, B_n, C_n, I_1, I_2, J_1, J_2, K_1, K_2, M$	variables defined for simplicity
b	short side of the channel
c_p	specific heat, J/kg K
k	thermal conductivity, W/m K
Kn	Knudsen number
N	normalization integral
Nu	Nusselt number, hD/k
Pr	Prandtl number, v/α
Q	heat flux, W/m^2
R	specific heat ratio
T	fluid temperature, K
u	fluid velocity, m/s
x, y, z	coordinate axes

Greek letters

α	thermal diffusivity, m^2/s
α'	a geometric definition, $\alpha' = (1+\gamma)/\gamma$
β_s	slip coefficient, $\beta_s = u_s/u_m$
γ	aspect ratio
λ	eigenvalues of the energy equation
λ_{mfp}	molecular mean free path, m
μ	eigenvalues of the momentum equation
ψ_m	eigenfunctions for the energy equation
ψ_n	eigenfunctions for the momentum equation
ρ	density, kg/m^3
θ	non-dimensional temperature

Subscript

b	bulk properties
m	average values
s	fluid properties at the wall
w	wall values
0	inlet properties

Superscripts

*	non-dimensional variables

applied to obtain the velocity distribution. For convenience, filtering schemes were also applied to obtain homogeneous boundary conditions [11]. Once the filtering is applied, the general procedure for the integral transform technique was followed. For velocity and temperature profiles, the same transform and inversion formulas were used.

To verify the method, the results for zero Knudsen number, which corresponds to a macrosize channel, were compared to the data from previous studies. Nu values for $Kn = 0$ are in good agreement with those given by Spiga and Morini [5] for all aspect ratios. A qualitative comparison between the results for non-zero Knudsen number and the microtube results was also made.

The analysis can easily be expanded for asymmetric heating conditions, for example, heating one side while insulating the others.

The amount of velocity slip and temperature jump was assumed to be the same at all boundaries and they were calculated at the bottom wall, $y = 0$. Throughout the analysis, the Prandtl number and gas constant were taken as 0.7 and 1.4, respectively. Since the value of the Prandtl number has a direct impact on the amount of temperature jump, $Pr = 0.6$ and $Pr = 0.9$ cases were also investigated.

2. Analysis

The geometry of the problem is given in Fig. 1. The center of the coordinate system is located at the bottom left corner of the channel. Heat flux at the wall is constant both axially and along the periphery. In the following two sections, the velocity and temperature profiles will be obtained analytically.

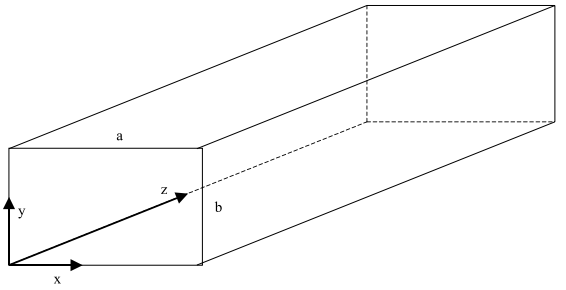

Fig. 1. The schematic of the problem.

2.1. Velocity profile

The incompressible momentum equation in the axial direction is solved to obtain the velocity distribution. Kavehpour et al. [12] solve the compressible forms of the momentum and energy equations with slip-flow considerations between two parallel plates. They find that the effect of compressibility is important for high Reynolds numbers and that the effect of rarefaction is significant for the lower Re. For a hydrodynamically developed flow in a rectangular channel, the conservation of momentum equation can be written in the following form:

$$\frac{1}{\mu}\frac{\partial P}{\partial z} = \frac{\partial^2 u}{\partial x^2} + \frac{\partial^2 u}{\partial y^2}, \tag{1}$$

and the boundary conditions can be written as follows based on the assumption that the slip velocity is constant and the same at each boundary

$$u = u_s \quad \text{at } x = 0 \text{ and } a;\ y = 0 \text{ and } b. \tag{2}$$

The governing equation and the boundary conditions are non-dimensionalized by the following parameters:

$$u^* = \frac{u}{u_m}, \quad x^* = \frac{x}{a}, \quad y^* = \frac{y}{a}. \tag{3}$$

Eq. (1) takes the following non-dimensional form:

$$P^* = \frac{\partial^2 u^*}{\partial x^{*2}} + \frac{\partial^2 u^*}{\partial y^{*2}} \tag{4}$$

and

$$u^* = \beta_s \quad \text{at } x^* = 0, 1 \text{ and } y^* = 0, \gamma,$$

where

$$P^* = \frac{a^2}{\mu u_m}\frac{\partial P}{\partial z}, \quad \beta_s = \frac{u_s}{u_m} \quad \text{and} \quad \gamma = \frac{b}{a},$$

where γ is the aspect ratio, β_s is the slip coefficient, which is the measure of the velocity slip at the boundary and P^* is the normalized pressure gradient. A similar definition of the slip coefficient is given by Shih et al. [13]. At the end of this section, the slip coefficient will be expressed in terms of the Knudsen number.

As seen from the above system of equations, the boundary conditions are non-homogeneous. Therefore, we are going to apply filtering to eliminate non-homogeneity. We define a one-dimensional problem in the y-direction such that it satisfies the boundary conditions of the original problem. Therefore, the velocity at the top and bottom walls vanishes for the original problem. We will also drop * for non-dimensional parameters.

$$u(x, y) = u_y(y) + \tilde{u}(x, y), \tag{5}$$

where u_y, filtering function, satisfies the following system:

$$\frac{d^2 u_y}{dy^2} - u_y = 0, \tag{6a}$$

$$u_y = \beta_s \quad \text{at } y = 0 \text{ and } y = \gamma, \tag{6b}$$

the solution of the above equation can easily be written as

$$u_y = \frac{e^y + e^{\gamma - y}}{1 + e^{\gamma}}\beta_s. \tag{7}$$

The governing equation and the boundary conditions take the following forms after the substitution of Eq. (5) into Eqs. (3) and (4):

$$P - u_y = \frac{\partial^2 \tilde{u}}{\partial x^2} + \frac{\partial^2 \tilde{u}}{\partial y^2}, \tag{8a}$$

$$\tilde{u} = \beta_s - u_y \quad \text{at } x = 0 \text{ and } x = 1, \tag{8b}$$

$$\tilde{u} = 0 \quad \text{at } y = 0 \text{ and } y = \gamma. \tag{8c}$$

We note here that, when the filtering scheme is applied, the boundary conditions must be written carefully to carry the changes along the computation. Now, we have two homogeneous and two non-homogeneous boundary conditions. We define the eigenvalue problem in the y-direction where we have the homogeneous boundary conditions, and then the other two will be implemented at the end. The appropriate eigenvalue problem and corresponding eigenvalues and eigenfunctions for the velocity problem are given in Table 1.

The transform and inversion formulas are written as:

$$\text{Transform} \quad \bar{\tilde{u}}(\mu_n, x) = \int_0^{\gamma} \frac{\psi_n(\mu_n, y)}{N_n^{1/2}} \tilde{u}(x, y)\, dy. \tag{9}$$

$$\text{Inversion} \quad \tilde{u}(x, y) = \sum_{n=1}^{\infty} \frac{\psi_n(\mu_n, y)}{N_n^{1/2}} \bar{\tilde{u}}(\mu_n, x). \tag{10}$$

The transformation process starts by applying $\int_0^{\gamma} \psi_n\, dy$ to every term in the governing equation

Table 1
The eigenvalue problems/solutions for momentum and energy equations

Eigenvalue problem	$y = 0$	$y = \gamma$	Eigenvalue, λ	Norm, N	Eigenfunction, ψ
Velocity distribution					
$\frac{d^2\psi_n}{dy^2} + \mu_n^2 \psi_n = 0$	$\psi_n = 0$	$\psi_n = 0$	$\mu_n = \frac{n\pi}{\gamma}$	$N_n = \frac{\gamma}{2}$	$\psi_n = \sin\left(\frac{n\pi}{\gamma} y\right)$
Temperature distribution					
$\frac{d^2\psi_m}{dy^2} + \lambda_m^2 \psi_m = 0$	$\frac{d\psi_m}{dy} = 0$	$\frac{d\psi_m}{dy} = 0$	$\lambda_m = \frac{m\pi}{\gamma}$	$N_m = \frac{\gamma}{2}$	$\psi_m = \cos\left(\frac{m\pi}{\gamma} y\right)$

$$\underbrace{\int_0^\gamma P\psi_n \,\mathrm{d}y}_{\mathrm{I}} - \underbrace{\int_0^\gamma u_y\psi_n \,\mathrm{d}y}_{\mathrm{II}} = \underbrace{\int_0^\gamma \frac{\partial^2\tilde{u}}{\partial x^2}\psi_n \,\mathrm{d}y}_{\mathrm{III}} + \underbrace{\int_0^\gamma \frac{\partial^2\tilde{u}}{\partial y^2}\psi_n \,\mathrm{d}y}_{\mathrm{IV}}. \tag{11}$$

The inversion and transform formulas, the eigenvalue problem and integration by parts technique are utilized to evaluate the integrals in Eq. (11). Therefore, Eq. (11) is obtained in the following transformed form:

$$\frac{\mathrm{d}^2\overline{\tilde{u}}}{\mathrm{d}x^2} - \mu_n^2\overline{\tilde{u}} = \frac{\gamma(1-(-1)^n)}{n\pi N_n^{1/2}}P - \frac{n\pi\gamma(1-(-1)^n)}{N_n^{1/2}(\gamma^2+n^2\pi^2)}\beta_s. \tag{12}$$

Transformation of the boundary conditions yields (9)

$$\overline{\tilde{u}} = \frac{(1-(-1)^n)}{N_n^{1/2}}\left(\frac{\gamma}{n\pi} - \frac{n\pi\gamma}{\gamma^2+n^2\pi^2}\right)\beta_s \quad \text{at } x=0 \text{ and } x=1. \tag{13}$$

The solution to the non-homogeneous ordinary differential equation, Eq. (12), is obtained analytically and, after some arrangements, put into the following appropriate form:

$$\overline{\tilde{u}} = K_1(\mu_n,x)P + K_2(\mu_n,x)\beta_s, \tag{14}$$

where

$$K_1 = \frac{B_n\,\mathrm{e}^{\mu_n x} + B_n\,\mathrm{e}^{-\mu_n(x-1)}}{1+\mathrm{e}^{\mu_n}} - B_n,$$

$$K_2 = \frac{A_n\,\mathrm{e}^{\mu_n x} + A_n\,\mathrm{e}^{-\mu_n(x-1)}}{1+\mathrm{e}^{\mu_n}} + C_n,$$

$$A_n = \frac{[1-(-1)^n]}{N_n^{1/2}}\left(\frac{\gamma}{n\pi} - \frac{n\pi\gamma}{\gamma^2+n^2\pi^2} - \frac{n\pi\gamma}{\mu_n^2(\gamma^2+n^2\pi^2)}\right),$$

$$B_n = \frac{\gamma[1-(-1)^n]}{\mu_n^2 n\pi N_n^{1/2}}, \quad C_n = \frac{n\pi\gamma[1-(-1)^n]}{\mu_n^2 N_n^{1/2}(\gamma^2+n^2\pi^2)}.$$

Then, the inversion formula is applied to obtain $\tilde{u}$

$$\tilde{u}(x,y) = \sum_n \times \frac{[K_1(\mu_n,x)P + K_2(\mu_n,x)\beta_s]\sin((n\pi/\gamma)y)}{N_n^{1/2}}. \tag{15}$$

The final form of the velocity profile is obtained by summing Eqs. (7) and (15). The value of P is still unknown in Eq. (15), which is obtained by implementing the definition of mean velocity

$$u_m = \frac{1}{ab}\int_0^b\int_0^a u(x,y)\,\mathrm{d}x\,\mathrm{d}y. \tag{16}$$

Once Eqs. (7) and (15) are substituted into Eq. (16), P is evaluated as follows:

$$P = \frac{1-(I_2+I_3)\beta_s}{I_1}, \tag{17}$$

where

$$I_1 = \frac{1}{\pi N_n^{1/2}}\sum_n \frac{[1-(-1)^n]}{n}\int_0^1 K_1(\mu_n,x)\,\mathrm{d}x,$$

$$I_2 = \frac{1}{\pi N_n^{1/2}}\sum_n \frac{[1-(-1)^n]}{n}\int_0^1 K_2(\mu_n,x)\,\mathrm{d}x,$$

$$I_3 = \frac{2(\mathrm{e}^\gamma-1)}{\gamma(\mathrm{e}^\gamma+1)}.$$

The only unknown left is the slip coefficient. We are going to obtain β_s as a function of the Knudsen number. We use the definition of slip velocity at the wall [7], which is given by

$$u_s = \lambda_{mfp}\left.\frac{\partial u}{\partial y}\right|_{y=0}. \tag{18}$$

Once the derivative of the velocity profile is evaluated at $y=0$ and set equal to u_s, the following expression for the slip coefficient, in non-dimensional form, is obtained. We note here that the average value of β_s is calculated by integrating over the length.

$$\beta_s = \int_0^1 \left\{\left\{\frac{\pi Kn}{N_n^{1/2}I_1}\sum_{n=1} nK_1\right\} \Big/ \left\{\gamma - \frac{Kn\gamma(1-\mathrm{e}^\gamma)}{(1+\mathrm{e}^\gamma)} + \frac{\pi Kn}{N_n^{1/2}}\sum_{n=1}\left(\frac{nK_1(I_2+I_3)}{I_1} - nK_2\right)\right\}\right\}\mathrm{d}x, \tag{19}$$

where the Knudsen number is $Kn = \lambda_{mfp}/a$.

The velocity profiles for $\gamma = 0.5$ and varying Knudsen numbers are shown in Fig. 2. As expected, for $Kn = 0$, velocity at the wall is zero. For increasing Kn, velocity slip at the wall also increases. Another observation that one can make is that the maximum velocity in the channel decreases, as the rarefaction effects become more significant. Maximum velocity is 1.9920 for $Kn = 0$, while it is 1.4208 for $Kn = 0.12$. We can also see that the magnitude of the slip velocity is the same along the boundary as defined by the boundary conditions.

The variation of the slip coefficient, non-dimensional slip velocity, with respect to the Knudsen number is given in Fig. 3. For the same Knudsen number, as the aspect ratio becomes smaller, the value of the slip coefficient increases. Table 2 shows slip coefficients for $0 \leqslant Kn \leqslant 0.12$ and $0.1 \leqslant \gamma \leqslant 1$.

2.2. Temperature profile

In the previous section, the fully developed velocity profile in a rectangular channel for various aspect ratios was determined. In this section we will attempt to obtain the fully developed temperature distribution for the same channels subjected to heat flux at all sides.

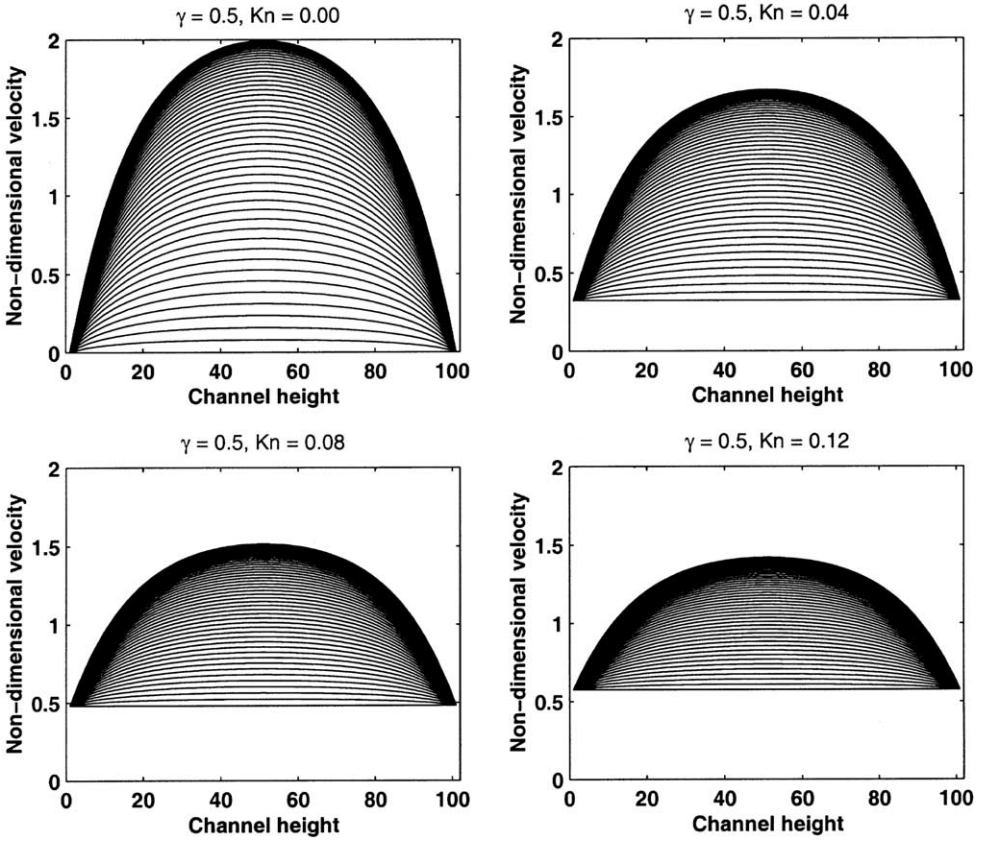

Fig. 2. Fully developed velocity profiles for different Knudsen numbers at $\gamma = 0.5$.

Then, the Nusselt number will be obtained for each case. We start with the conservation of the energy equation for a thermally fully developed flow in a rectangular channel.

$$u\frac{\partial T}{\partial z} = \alpha\left(\frac{\partial^2 T}{\partial x^2} + \frac{\partial^2 T}{\partial y^2}\right) \tag{20a}$$

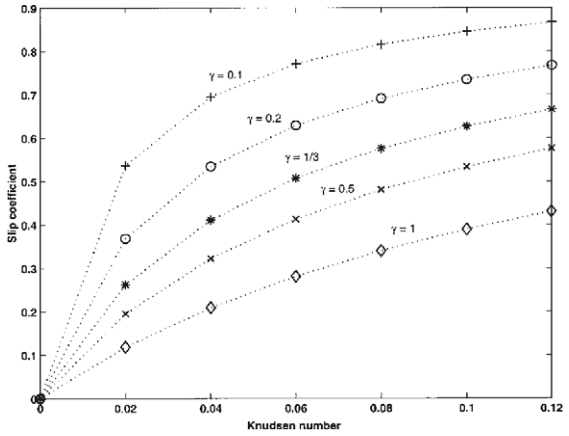

Fig. 3. The variation of slip coefficient with Knudsen number.

and the boundary conditions are:

$$-k\frac{\partial T}{\partial x} = q \quad \text{at } x = 0, \tag{20b}$$

$$k\frac{\partial T}{\partial x} = q \quad \text{at } x = a, \tag{20c}$$

$$-k\frac{\partial T}{\partial y} = q \quad \text{at } y = 0, \tag{20d}$$

$$k\frac{\partial T}{\partial y} = q \quad \text{at } y = b. \tag{20e}$$

The left-hand side of Eq. (20a) can be approximated as [4,5]

$$\frac{\partial T}{\partial z} = \frac{q(2a+2b)}{\rho c_p u_m ab}$$

for fully developed flow in a rectangular channel heated at all boundaries.

The energy equation and associated boundary conditions are non-dimensionalized by the same parameters. The non-dimensional form of the energy equation is then obtained as

$$u^*\left(\frac{1+\gamma}{\gamma}\right)^2 = \frac{\partial^2\theta}{\partial x^{*2}} + \frac{\partial^2\theta}{\partial y^{*2}}, \tag{21a}$$

Table 2
The value of the slip coefficient for varying γ and Kn

Kn	γ									
	1	0.834	0.75	0.667	0.5	0.334	0.25	0.2	0.125	0.1
0	0	0	0	0	0	0	0	0	0	0
0.02	0.12	0.13	0.14	0.16	0.2	0.26	0.32	0.37	0.48	0.54
0.04	0.21	0.23	0.25	0.27	0.32	0.41	0.48	0.53	0.65	0.69
0.06	0.28	0.31	0.33	0.35	0.41	0.51	0.58	0.63	0.73	0.77
0.08	0.34	0.37	0.39	0.42	0.48	0.58	0.64	0.69	0.78	0.82
0.1	0.39	0.42	0.44	0.47	0.53	0.63	0.69	0.73	0.81	0.85
0.12	0.43	0.47	0.49	0.51	0.58	0.67	0.73	0.77	0.84	0.87

Table 3
Filtering functions for the energy equation

	Governing equation	Boundary condition $x=0,\ y=0$	Boundary condition $x=1,\ y=\gamma$	Solution
X-filtering	$\frac{d^2\theta_x}{dx^2}-\theta_x=0$	$\frac{d\theta_x}{dx}=-\frac{\alpha'}{2}$	$\frac{d\theta_x}{dx}=\frac{\alpha'}{2}$	$\theta_x=\frac{\alpha'}{2}\left(\frac{1}{e-1}e^{x}+\frac{e}{e-1}e^{-x}\right)$
Y-filtering	$\frac{d^2\theta_y}{dy^2}-\theta_y=0$	$\frac{d\theta_y}{dy}=-\frac{\alpha'}{2}$	$\frac{d\theta_y}{dy}=\frac{\alpha'}{2}$	$\theta_y=\frac{\alpha'}{2}\left(\frac{1}{e^{\gamma}-1}e^{y}+\frac{e^{\gamma}}{e^{\gamma}-1}e^{-y}\right)$

where

$$\theta=\frac{T-T_0}{(qD_h/k)},$$

with the following non-dimensional boundary conditions:

$$\frac{\partial\theta}{\partial x^*}=-\frac{a}{D_h}\quad \text{at } x^*=0, \tag{21b}$$

$$\frac{\partial\theta}{\partial x^*}=\frac{a}{D_h}\quad \text{at } x^*=1, \tag{21c}$$

$$\frac{\partial\theta}{\partial y^*}=-\frac{a}{D_h}\quad \text{at } y^*=0, \tag{21d}$$

$$\frac{\partial\theta}{\partial y^*}=\frac{a}{D_h}\quad \text{at } y^*=\gamma. \tag{21e}$$

Similar to the previous case, the boundary conditions are non-homogeneous. In this case, for convenience, we define a filtering function in each direction to make the heat flux zero (homogeneous boundary conditions). First, the temperature is written as

$$\theta(x,y)=\theta_x(x)+\theta_y(y)+\tilde{\theta}(x,y), \tag{22}$$

where θ_x and θ_y are obtained similar to the u_y of the velocity profile and given in Table 3, where $\alpha'=(1+\gamma)/\gamma$. Now, we go back to the governing equation and substitute equation (22)

$$\frac{\partial^2\tilde{\theta}}{\partial x^2}+\frac{\partial^2\tilde{\theta}}{\partial y^2}=u\alpha'^2-\theta_x-\theta_y, \tag{23a}$$

with the following homogeneous boundary conditions:

$$\frac{\partial\tilde{\theta}}{\partial x}=0\quad \text{at } x=0 \text{ and } x=1, \tag{23b}$$

$$\frac{\partial\tilde{\theta}}{\partial y}=0\quad \text{at } y=0 \text{ and } y=\gamma. \tag{23c}$$

The integral transform technique is again applied to solve for temperature. The appropriate eigenvalue problem and solution to this problem are shown in Table 1. The transform and inversion formulas are the same as in the velocity problem. We multiply every term in Eq. (23a) by $\int_0^{\gamma}\psi_m\,dy$ to start the transformation process. After some simplifications, the transformed equation is obtained as follows:

$$\frac{d^2\bar{\tilde{\theta}}}{dx^2}-\lambda_m^2\bar{\tilde{\theta}}=\frac{\alpha'^2}{N_m^{1/2}N_n^{1/2}}\sum_{n=1,3}^{\infty}[K_1(\mu_n,x)I+K_2(\mu_n,x)\beta_s]D(m,n)+J_m-P_m, \tag{24a}$$

where D, P_m and J_m are defined as

$$D=\int_0^{\gamma}\sin\left(\frac{n\pi y}{\gamma}\right)\cos\left(\frac{m\pi y}{\gamma}\right)dy=\begin{cases}\frac{\gamma n\left[(-1)^{n+m}-1\right]}{\pi(m^2-n^2)} & \text{for } m\neq n,\\ 0 & \text{for } m=n,\end{cases}$$

$$P_m=\frac{\alpha'}{2N^{1/2}}\int_0^{\gamma}\left(\frac{1}{e^{\gamma}-1}e^{y}+\frac{e^{\gamma}}{e^{\gamma}-1}e^{-y}\right)\cos\left(\frac{m\pi y}{\gamma}\right)dy$$

and

$$J_m = \frac{\gamma^2 \alpha'^2 \beta_s (e^{\gamma} - 1)((-1)^m + 1)}{(e^{\gamma} + 1)(\gamma^2 + m^2\pi^2) N_m^{1/2}},$$

and the required boundary conditions to solve the transformed system are given as:

$$\frac{d\bar{\bar{\theta}}}{dx} = 0 \quad \text{at } x = 0 \text{ and } x = 1. \tag{24b}$$

Eq. (24a) is first solved for the homogeneous case (no source term), and the particular solution is obtained by considering the right-hand side. These two solutions are added to each other to yield

$$\begin{aligned}\bar{\bar{\theta}}(\lambda_m, x) = {} & \left(\frac{M}{\lambda_m(e^{\lambda_m} - 1)}\right) e^{\lambda_m x} \\ & + \left(\frac{M e^{\lambda_m}}{\lambda_m(e^{\lambda_m} - 1)}\right) e^{-\lambda_m x} + \frac{\alpha'^2}{2\lambda_m N_m^{1/2} N_n^{1/2}} \\ & \times \sum_{n=1,3}^{\infty} \left[\frac{2\lambda_m J_1 (e^{\mu_n x} + e^{\mu_n} e^{-\mu_n x})}{(\mu_n^2 - \lambda_m^2)} \right. \\ & \left. - \frac{2J_2}{\lambda_m} \right] D_{mn} - \frac{J_m}{\lambda_m^2} + \frac{P_m}{\lambda_m^2},\end{aligned} \tag{25}$$

where the integration constant is given as

$$M = \frac{\alpha'^2}{N_m^{1/2} N_n^{1/2}} \sum_{n=1,3}^{\infty} D_{mn} \left[\frac{J_1 \mu_n (1 - e^{\mu_n})}{(\mu_n^2 - \lambda_m^2)} \right]$$

and

$$J_1 = \frac{B_n I + A_n \beta_s}{1 + e^{\mu_n}} \quad \text{and} \quad J_2 = C_n \beta_s - B_n I.$$

To obtain the temperature profile, the inversion formula is applied to Eq. (25), and θ_x and θ_y are added to it. The values for bulk mean temperature and average wall temperatures are needed to calculate the Nusselt number. Bulk temperature is defined as

$$\theta_b = \frac{1}{\gamma} \int_0^{\gamma} \int_0^1 u(x,y)\theta(x,y)\,dx\,dy,$$

fand the average wall temperature is obtained from the following relation [5]:

$$\theta_w = \frac{\int_0^1 \theta(x,0)\,dx + \int_0^1 \theta(x,\gamma)\,dx + \int_0^{\gamma} \theta(0,y)\,dy + \int_0^{\gamma} \theta(1,y)\,dy}{2(1+\gamma)}.$$

If there was no temperature jump at the wall, the Nusselt number would be calculated using

$$Nu = \frac{1}{\theta_w - \theta_b}. \tag{26}$$

Table 4
Fully developed Nusselt number for $0 \leqslant Kn \leqslant 0.12$ and $0.1 \leqslant \gamma \leqslant 1$ at $Pr = 0, 6; 0.7; 0.9$

Kn	*Pr*	γ									
		1	0.84	0.75	0.67	0.5	0.34	0.25	0.2	0.125	0.1
0	0.6	3.1	3.09	3.08	3.07	3.03	2.96	2.93	2.9	2.85	2.82
	0.7	3.1	3.09	3.08	3.07	3.03	2.96	2.93	2.9	2.85	2.82
	0.9	3.1	3.09	3.08	3.07	3.03	2.96	2.93	2.9	2.85	2.82
0.02	0.6	2.95	2.93	2.92	2.9	2.85	2.76	2.67	2.59	2.35	2.19
	0.7	2.99	2.98	2.98	2.97	2.92	2.85	2.78	2.71	2.49	2.34
	0.9	3.07	3.06	3.58	3.05	3.02	2.97	2.93	2.88	2.72	2.59
0.04	0.6	2.76	2.73	2.71	2.68	2.59	2.42	2.27	2.12	1.75	1.56
	0.7	2.85	2.82	2.81	2.79	2.71	2.56	2.42	2.28	1.92	1.72
	0.9	2.98	2.97	2.96	2.94	2.88	2.77	2.66	2.54	2.2	2
0.06	0.6	2.58	2.53	2.5	2.46	2.33	2.11	1.92	1.75	1.37	1.19
	0.7	2.69	2.65	2.62	2.59	2.48	2.27	2.09	1.91	1.52	1.33
	0.9	2.86	2.84	2.82	2.79	2.7	2.53	2.36	2.2	1.79	1.59
0.08	0.6	2.4	2.34	2.3	2.25	2.1	1.85	1.64	1.47	1.11	0.95
	0.7	2.53	2.48	2.44	2.4	2.26	2.02	1.81	1.63	1.25	1.08
	0.9	2.74	2.7	2.67	2.63	2.52	2.29	2.09	1.91	1.5	1.31
0.10	0.6	2.23	2.17	2.12	2.06	1.91	1.64	1.43	1.27	0.94	0.79
	0.7	2.38	2.32	2.28	2.22	2.07	1.81	1.59	1.42	1.06	0.9
	0.9	2.61	2.56	2.52	2.48	2.34	2.09	1.87	1.68	1.29	1.11
0.12	0.6	2.05	2.01	1.96	1.9	1.74	1.47	1.27	1.11	0.81	0.69
	0.7	2.24	2.17	2.12	2.06	1.9	1.63	1.42	1.25	0.92	0.78
	0.9	2.49	2.43	2.38	2.33	2.18	1.9	1.68	1.5	1.12	0.96

In the presence of such a difference between the fluid and the wall temperatures, we use the following relation:

$$Nu = 1 \Big/ \left\{ \theta_s + \frac{2R}{1+R} \frac{\alpha'}{2} \frac{Kn}{Pr} - \theta_b \right\}, \tag{27}$$

where the temperature jump at the wall for Cartesian coordinates is given as [7]:

$$T_s - T_w = \frac{2R}{1+R} \frac{\lambda_{mfp}}{Pr} \left. \frac{\partial T}{\partial y} \right|_{y=0}, \tag{28}$$

which takes the following non-dimensional form with $\partial\theta/\partial y|_{y=0} = -(a/D_h)$:

$$\theta_s - \theta_w = -\frac{2R}{1+R} \frac{\alpha'}{2} \frac{Kn}{Pr}. \tag{29}$$

3. Results and discussion

The effects of rarefaction and channel size on the velocity distribution were shown at the end of the previous section. In this section, we are going to discuss the same effects for the heat transfer. The fully developed Nusselt number values are given also in Table 4 for all different cases considered here.

In Fig. 4, the effect of *Kn* on heat transfer for varying aspect ratios is shown. As seen in the figure, when *Kn* increases the Nusselt number decreases, regardless of the value of the aspect ratio, due to the increasing temperature jump. However the decrease in *Nu* is more significant for smaller values of γ. Going from $Kn = 0$ to $Kn = 0.12$ causes a 31% decrease in *Nu* for $\gamma = 1$, whereas the decrease is 72.4% for $\gamma = 0.1$. This behavior may also be explained by the increasing rarefaction as the channel size is reduced.

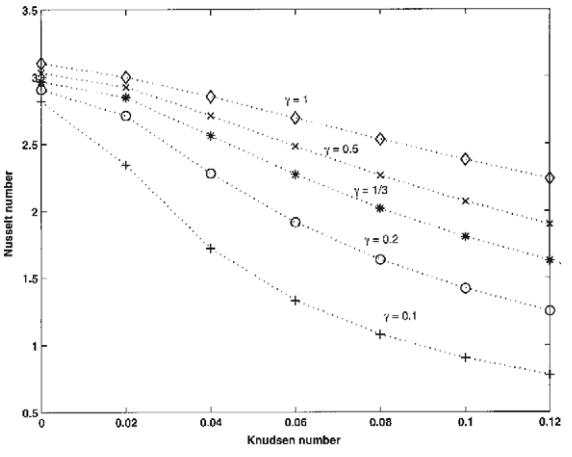

Fig. 4. The effect of Knudsen number on fully developed Nusselt number for varying aspect ratios.

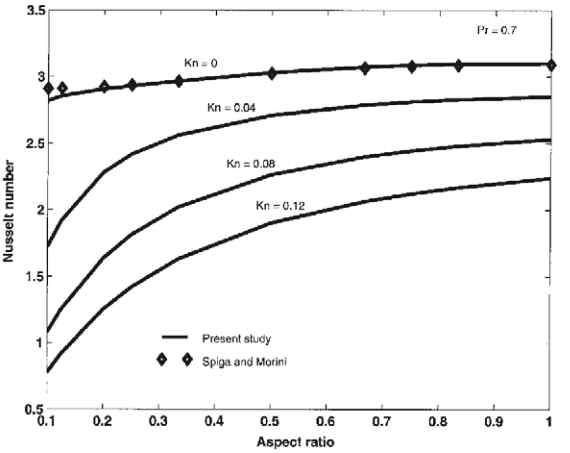

Fig. 5. The effect of channel size on the Nusselt number for varying *Kn*.

The effect of channel size can also be seen in Fig. 5. The size effects become more significant when the aspect ratio drops below 0.5. This can be explained from the mathematical viewpoint: α' in Eq. (29) takes higher values as γ decreases which increases the temperature jump. For example, while $\alpha' = 1$ for $\gamma = 1$, it is 5.5 for $\gamma = 0.1$. The results for zero Knudsen, a conventionally sized channel, are also compared to the results from Spiga and Morini [5] for the same boundary conditions. They show a good agreement except for very small values of the aspect ratio.

When the temperature jump is not taken into account, in other words, only the effect of velocity slip is considered, the Nusselt number increases with increasing Knudsen numbers. The results are seen in Fig. 6. In this case, the increment is larger for smaller channels due to

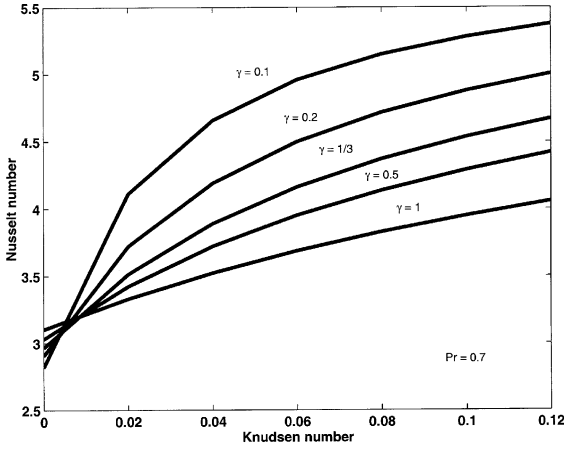

Fig. 6. Variation of the fully developed Nusselt number with Knudsen number without considering temperature jump at the wall.

the increase in the magnitude of the slip velocity. The same behavior was found for microtubes by several researchers [8,9].

The effect of the Prandtl number can be seen in Table 4. Besides the fact that Pr increases Nu by reducing the temperature jump, it should be noted that as the aspect ratio decreases, the change in Nu due to Pr is amplified. Nu changes 17.7% from $Pr = 0.6$ to $Pr = 0.9$ for $\gamma = 1$, while the amount of change is 28.1% for $\gamma = 0.1$.

Viscous heating is not considered in this analysis. In their recent paper, Tunc and Bayazitoglu [10] show the effects of viscous dissipation for a cylindrical microchannel. In the current analysis, the obtained Nusselt number variation with the Knudsen number is similar to the one given in [10] for a cylindrical geometry. Therefore, one can expect the effect of viscous heating in a rectangular channel to be the same as the effect in a cylindrical one.

References

[1] E.B. Arkilic, K.S. Breuer, M.A. Schmidt, Gaseous flow in microchannels, in: Application of Microfabrication to Fluid Mechanics, ASME FED, 197, 1994, pp. 57–66.

[2] J.C. Shih, C. Ho, J. Liu, Y. Tai, Monatomic and polyatomic gas flow through uniform microchannels, in: 1996 National Heat Transfer Conference, Micro Electro Mechanical Systems (MEMS), Atlanta, GA, DSC 59 (1996) 197–203.

[3] A. Beskok, G.E. Karniadakis, Simulation of heat and momentum transfer in complex micro geometries, J. Ther. Heat Transfer 8 (4) (1994) 647–653.

[4] S.X. Gao, J.P. Hartnett, Analytical Nusselt number predictions for slug flow in rectangular ducts, Int. Comm. Heat Mass Transfer 20 (5) (1993) 751–760.

[5] M. Spiga, G.L. Morini, Nusselt numbers in laminar flow for H2 boundary conditions, Int. J. Heat Mass Transfer 39 (6) (1996) 1165–1174.

[6] G.L. Morini, Analytical determination of the temperature distribution and Nusselt numbers in rectangular ducts with constant axial heat flux, Int. J. Heat Mass Transfer 43 (2000) 741–755.

[7] R.F. Barron, X. Wang, T.A. Ameel, R.O. Warrington, The Graetz problem extended to slip-flow, Int. J. Heat Mass Transfer 40 (8) (1997) 1817–1823.

[8] E.M. Sparrow, S.H. Lin, Laminar heat transfer in tubes under slip-flow conditions, J. Heat Transfer 84 (1962) 363–369.

[9] T.A. Ameel, R.F. Barron, X. Wang, R.O. Warrington, Laminar forced convection in a circular tube with constant heat flux and slip flow, Microscale Thermophys. Eng. 1 (4) (1997) 303–320.

[10] G. Tunc, Y. Bayazitoglu, Heat transfer for gaseous flow in microtubes with viscous heating, Proc. ASME Heat Transfer Div., HTD 366-2 (2000) 299–306.

[11] R.M. Cotta, M.D. Mikhailov, Heat Conduction: Lumped Analysis, Integral Transforms, Symbolic Computation, Wiley, New York, 1997.

[12] H.P. Kavehpour, M. Faghri, Y. Asako, Effects of compressibility and rarefaction on gaseous flows in microchannels, Numer. Heat Transfer Part A 32 (1997) 677–696.

[13] Y.P. Shih, C.C. Huang, S.Y. Tsay, Extended leveque solution for laminar heat transfer to power-law fluids in pipes with wall slip, Int. J. Heat Mass Transfer 38 (3) (1995) 403–408.